ACS Photonics

pubs.acs.org/journal/apchd5

Article

Charge State Manipulation of NV Centers in Diamond under Phonon-Assisted Anti-Stokes Excitation of NV^0

Yuan-Fei Gao, Jia-Min Lai, Yu-Jia Sun, Xue-Lu Liu, Chao-Nan Lin, Ping-Heng Tan, Chong-Xin Shan,* and Jun Zhang*

Cite This: *ACS Photonics* 2022, 9, 1605−1613

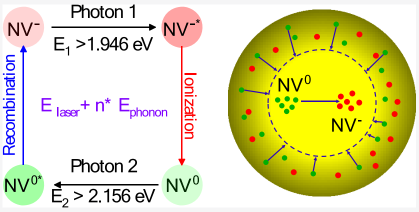

ABSTRACT: The manipulation of the charge states of nitrogen-vacancy (NV) centers in diamond is a prerequisite for next-generation quantum sensing, communication, and computing. Here, we use phonon-assisted anti-Stokes excitation to realize the reversible conversion between the NV^0 and NV$^-$ states. In this case, we observe two decay processes of NV$^-$ centers with lifetimes as long as tens of seconds. By studying the kinetics of spectral structure evolution of NV$^-$ states, we find that the spectral structure of the NV$^-$ center is modulated by the charge state transition process under anti-Stokes excitation. We propose that the main reason is the local electric field generated by the ionization of the NV$^-$, which changes the radiation environment of the color centers. Our results might provide an alternative method to control the charge states of nitrogen-vacancy centers.

KEYWORDS: *diamond, charge state control, phonon-assisted up-conversion, quantum optics*

INTRODUCTION

The color centers in diamond are potential candidates for next-generation solid-state quantum devices due to their excellent optical properties.[1−3] Being placed in a spin-free lattice, the negatively charged nitrogen-vacancy (NV$^-$) center shows the ultralong room-temperature spin dephasing times ever observed in solid-state systems.[4,5] The detection and manipulation of NV$^-$ centers in diamond have attracted tremendous interest as they lead to innovative applications in various domains of high-speed quantum electronic devices, nanoscale magnetic detection, and temperature sensing.[6,7] To enhance the sensitivity of NV$^-$ based quantum devices and the signal to noise ratio, a high concentration of NV$^-$ centers near the surface of the diamond is required. However, in most cases, the neutral charge state (NV^0) of NV centers is found close to the diamond surface,[8] but it lacks the required spin and optical properties of NV$^-$. Several methods have been used to solve this problem. In terms of diamond growth, the current methods for forming NV$^-$ centers in diamond are chemical vapor deposition (CVD),[9] N$^+$ ion implantation,[10] detonation,[11] and high-pressure high-temperature (HPHT) techniques.[12] The CVD process produces large-grain polycrystalline films where the nitrogen concentration is limited by thermodynamic solubility and large graphitic content.[13] Using the N$^+$ ion implantation technique, Frenkel defects and sp^2-bonded carbon will be formed, which is a challenge for annealing. Detonation and HPHT processes usually introduce other impurities and defects,[14,15] such as irons. In addition to controlling the growth process, other methods also have been studied, including surface hydrogenation or oxidation,[16] electric manipulation,[17,18] and optical control methods.[19] Ab initio calculation of the energy level structure of NV centers in bulk single-crystalline diamond reveals the impact of surface proximity on its complexity.[20,21] Specifically, it is found that typical diamond surfaces contain donor and acceptor states with sub-bandgap energy, which compromise the photostability of the NV centers by hybridization with the point defect gap states. This is the fundamental reason for adjusting the distribution of charge states by surface hydrogenation or oxidation.[16] In addition to the chemical properties of the diamond surface, the photoluminescence (PL) emission of NV centers strongly depends on the excitation wavelength.[22] The difference between the NV^0 and NV$^-$ states is whether to carry extra electrons. The optical control method provides a bidirectional switching between NV^0 and NV$^-$ states of the diamond. They control the occupation of carriers on the electronic energy level of the NV color centers by two different laser excitations.[23] In this method, the NV^0 state is converted to the NV$^-$ state under the excitation with low-power near-infrared (1064 nm) and visible (532 nm) lasers, resulting in increased PL of the NV$^-$ state.[24] Compared to other methods, the optical control method is convenient and reversible.

However, few reports have focused on the effect of phonon-assisted anti-Stokes photoluminescence (ASPL) up-conversion on the dynamics of NV centers. Compared to Stokes

Received: December 15, 2021
Published: April 26, 2022

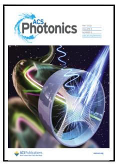

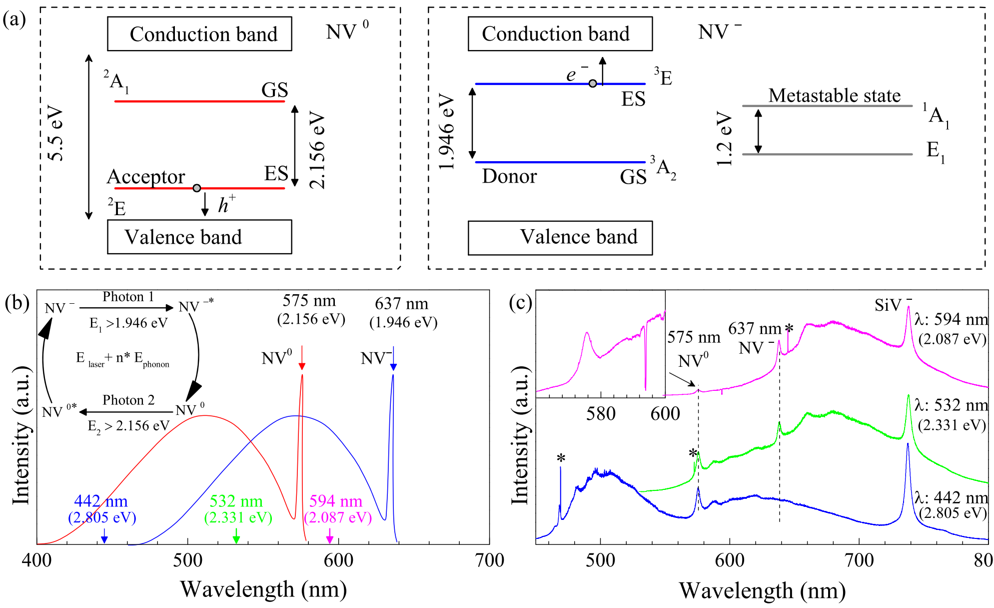

Figure 1. The transition process of nitrogen-vacancy centers (NVs) under different excitation lasers. (a) Simplified electronic energy schemes of the NVs. (b) The charge conversion process. Schematic representation of the absorption spectra of NV$^-$ (blue) and NV^0 (red). Phonon-assisted up-conversion of NV^0 excited by a 594 nm laser corresponds to the joint absorption of both charge states, where continuous charge switching and, therefore, efficient NV luminescence are possible. (c) PL and ASPL of NV centers in diamond. The sharp Raman peak at 1332 cm^{-1} is labeled in asterisks. PL spectra of NV centers excited at 442, 532, and 594 nm. The ASPL of NV^0 (575 nm) excited at 594 nm is shown in the inset for clarity.

excitation, the thermal energy (phonons) contained in materials is taken away by the emitted anti-Stokes photons during the ASPL process, so that the ASPL process can achieve laser cooling of phonons and materials.[25−27] The phonon-assisted anti-Stokes excitation process can effectively suppress the thermal effect on the electrons and has been extensively studied in many areas such as cavity quantum electrodynamics,[28] optical refrigeration,[25] and bioimaging.[29] Quantum emitters in solids are at the forefront of quantum information science and quantum sensing owing to their robustness, ease of handling, and prospects for scalability.[30] However, a notable majority of these emitters exhibit spectral diffusion due to local, fluctuating electromagnetic fields, which hinder their applicability in practical applications.[31] The energy instability is detrimental to the coherence of the emitted photons, and, thus, to the quality of two- or multiphoton entanglement.[32] Approaches toward mitigating this undesired phenomenon include improving the purity of the host materials to minimize foreign defect sites,[33] changing the defect symmetry,[34] depleting the noise sources,[35] or employing active energy stabilization strategies to induce a dynamic Stark shift via external electric fields.[36] Recently, Tran et al.[37] demonstrated efficient anti-Stokes excitation of color centers in hexagonal boron nitride and found that this process suppressed the spectral diffusion of quantum emitters. Also, Wang et al.[38] reported that the coherent control of solid-state spin bits in SiC under anti-Stokes excitation, which has higher optically detected magnetic resonance (ODMR) contrast than that under Stokes excitation, implying that anti-Stokes excitation is expected to provide more promising properties for defect centers. Therefore, it is of great significance to study the anti-Stokes excitation during the charge state conversion process of NV centers in diamond for the application of the color center in solid-state single-photon sources.

In this work, we realize the reversible manipulation of the charge states of the NV center by using phonon-assisted anti-Stokes excitation. We observe two decay processes of the NV$^-$ center by investigating the ASPL dynamics of the NV$^-$ center. Furthermore, we find that the spectral structure of the NV$^-$ center could be modulated by the charge state conversion process under anti-Stokes excitation.

RESULTS AND DISCUSSION

The charge dynamics of NV states under optical excitation can be understood with the aid of energy diagrams in Figure 1a,b: by absorbing one photon with energy greater than 2.6 eV (i.e., 477 nm) or two photons with energy greater than 1.946 eV (i.e., 637 nm) in succession, the electron of the negatively charged NV$^-$ is excited to the conduction band, so that NV$^-$ is ionized into NV^0.[39] In the mechanism of two-photon successive absorption, the first photon pumps NV$^-$ to its first excited state, and the second photon excites the electron into the conduction band. Similarly, NV^0 can be photoconverted back to NV$^-$ either via a single-photon absorption (for energies >2.94 eV (422 nm)) or by a two-step process involving pushing the hole into the excited state by absorption of a photon with energy >2.156 eV (i.e., 575 nm), and exciting the hole to the valence band by second photon. Note that with the above constraints, red (632 nm) laser illumination mostly results in a unidirectional charge conversion process, i.e., from NV$^-$ into NV^0, while the reverse process is mostly suppressed. By contrast, green (532 nm) laser excitation dynamically modulates the NV state between negative and neutral charged states. At this wavelength, the population of equilibrium NV$^-$ is approximately 75%.[39] However, in addition to using photons to achieve a closed-loop, the phonon is also expected to achieve the reversible conversion between NV^0 and NV$^-$. When excited by a 594 nm (2.087 eV) laser, the phonon-assisted ASPL up-conversion happens because of the thermal occupation of phonons in the electronic ground state. In other words, the neutral charge state NV^0 could absorb a photon and phonons and then transform from the ground state into the

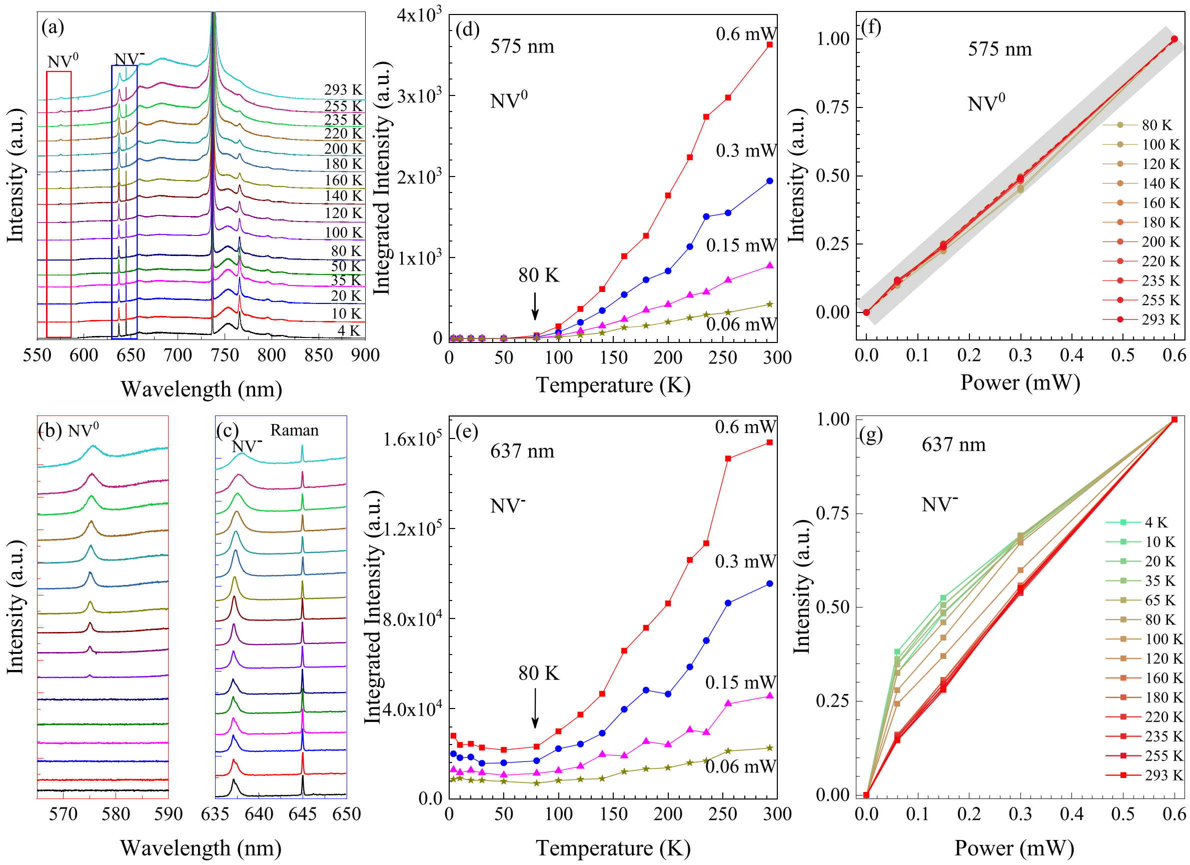

Figure 2. Temperature and laser power dependence of NV^0 and NV$^-$ emissions. (a) PL spectra excited by a 594 nm laser with a power of 0.6 mW at different temperatures. (b, c) Magnification of ZPL of NV^0 and NV$^-$ as a function of temperature, respectively. (d, e) Temperature dependences of the total intensity for NV^0 and NV$^-$ excited by 594 nm with different powers, respectively. (f, g) Power dependence of PL intensities for NV^0 and NV$^-$ at different temperatures, respectively.

excited state. Thus, the laser wavelength at 594 nm is within the combined absorption range of the two charged states, allowing continuous charge switching and effective NV$^-$ luminescence. When both excited states of NV color centers appear at the center of the laser spot, the PL of NV^0 and NV$^-$ can be observed simultaneously. The Stokes PL and ASPL spectra of NV centers excited by 442, 532, and 594 nm lasers were measured at room temperature. As shown in Figure 1c, several optical peaks are observed. The very sharp Raman peak at 1332 cm^{-1} (labeled as asterisks) comes from a zone-center optical phonon in diamond, which means good crystalline quality. The peak at around 737 nm is the zero phonon lines (ZPL) of SiV$^-$ centers.[40] The peaks at 575 and 637 nm are the ZPL of the neutral charge state (NV^0) and negative charge state (NV$^-$), respectively.[41] As we expected, we simultaneously observed the PL of NV^0 and NV$^-$ under excitation of 532 and 594 nm, while only PL of NV^0 was observed under the excitation condition of 442 nm.

To assess the effect of phonons on charge conversion, it is necessary to confirm whether the process originates from phonon assistance. Similar to ASPL up-conversion of the SiV$^-$ color centers,[26] the anti-Stokes PL in NV color centers caused by phonon-assisted up-conversion and two-photon absorption mechanism exhibit completely different phenomena with temperature changes.[25] ASPL efficiency depends on the average phonon population and external quantum efficiency. The average phonon population increases exponentially with temperature, while the external quantum efficiency is almost unchanged at low temperatures and decreases at higher temperatures because of the enhancement of nonradiative recombination.[42] However, the two-photon absorption fluorescence up-conversion is mainly affected by the external quantum efficiency, so it should be easier to observe at low temperatures. Therefore, we measured the temperature-dependent PL spectra under 594 nm excitation. During the measurements, we observed that the luminescence intensity of the negative charge state NV$^-$ decays with time. Thus, we measured the spectra under the steady state after continuous illumination for 300 s. Figure 2a shows the PL spectra at different temperatures. Here, the energy of the laser is 2.087 eV (<2.516 eV), which cannot support the abovementioned two-photon absorption from NV^0 to NV$^-$. Thus, the ASPL or two-photon absorption occurs in the process from the ground state to the excited state of NV^0.

For clarity, the ZPL of NV^0 and NV$^-$ is magnified in Figure 2b,c. The PL spectra at different temperatures were normalized by the Raman peak of the diamond (1332 cm^{-1}) because it is not sensitive to temperature.[43] We extracted the PL intensity of NV^0 and NV$^-$ from the temperature-dependent PL spectra under different excitation powers as shown in Figure 2d,e. The luminescence of the neutral charge state NV^0 (575 nm) could be observed above 80 K, and it rises rapidly with the increase of temperature, which is consistent with the trend of APSL.[26] When the temperature rises to 240 K, the external quantum efficiency significantly decreases while the increase of the up-conversion efficiency is caused by the increases in the average

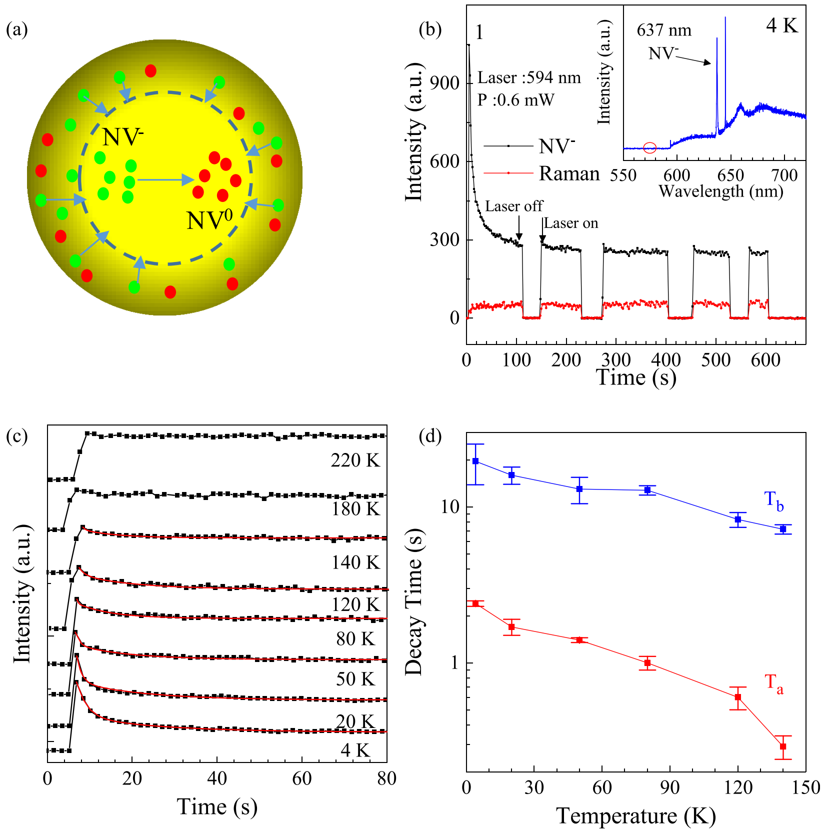

Figure 3. Charge state transition of NV color centers at different temperatures. (a) Schematic diagram of the laser spot on the surface. The green and red balls represent the NVs in the negative and neutral charge states, respectively. The area within the dotted line represents the central area of the light spot. (b) The decay process of the NV^- color centers' PL with time at 4 K excited by the 594 nm laser. The inset shows the PL spectrum at 4 K. The lasers were switched alternately during the measurement process. Leaving the sample without optical irradiation for several minutes will not change the level of PL intensity. (c) NV^- PL decay process with time at different temperatures. The sampling interval is about 1.5 s. The black dots and red solid plots represent the experimental data and the double exponential decay fitting curves, respectively. (d) Temperature dependence of decay parameters T_a and T_b.

population of phonon, so the ASPL intensity starts to deviate from the exponential function above 240 K.[42] Based on this phenomenon, we can initially confirm that the process is phonon-assisted ASPL up-conversion rather than two-photon absorption.

We observed three processes for NV^- in which the intensity decreases slightly first, rises to the maximum, and decreases in the end in Figure 2e. In the range between 4 and 80 K, the mean number of phonons is too low for the phonon-assisted up-conversion process of NV^0 to occur, and only a unidirectional process of NV^- to NV^0 occurs. When the temperature rises to 80 K, the phonon-assisted ASPL up-conversion process of NV^0 satisfies the closed-loop condition in Figure 1b. The total NV states including NV^0 and NV^- at the center of the laser spot establish a new balance like 532 nm excitation. Under closed-loop conditions, the NV color center tends to remain in a negatively charged state,[22] so the PL intensity continues to increase. When the temperature reaches 200 K, the external quantum efficiency is significantly reduced, resulting in the intensity decline.[42] Therefore, we confirm that this is due to the phonon-assisted ASPL up-conversion that satisfies the closed-loop condition, resulting in abnormal behavior for NV^-. The thermal activation during the heating process may affect the conversion process of the charge state, but the concentration of shallow-level impurities in the samples grown by MPCVD is relatively low. Even at room temperature, the electron occupation of the conduction band is very little; thus, the thermal activation of carriers is ignorable in our experiments. When pumping on the sideband, a nonlinear stimulated emission process may occur.[44,45] Considering the limitation of the relatively low-power laser we used, the stimulated emission process can be ignored in our experiments. Limited by the excitation wavelength, we only show the experiments under 594 nm. The phonon-assisted ASPL intensity follows the phonon population function $(e^{\Delta E/k_BT} - 1)^{-1}$, where ΔE is up-conversion energy defined as the energy difference between the luminescence of NV^0 and the pump laser. Rigorous experiments require the determination of phonon sidebands by absorption or photoluminescence excitation spectroscopy. Theoretically, as the red-detuning energy between the excitation light and the zero phonon line increases, the probability of phonon-assisted up-conversion decreases exponentially. When the loop is broken, we can only observe the PL decay process of the NV^-.

In addition to PL intensity, we also observe an abnormal behavior in the power dependence of NV^- in Figure 2g. At low temperatures, the saturation phenomenon appears, and as the temperature increases, it gradually changes to a linear dependence on the laser power. We believe that the transition from NV^- to NV^0 at the center of the laser spot is a unidirectional charge conversion process at low temperature,[46] which causes a significant reduction of the concentration of

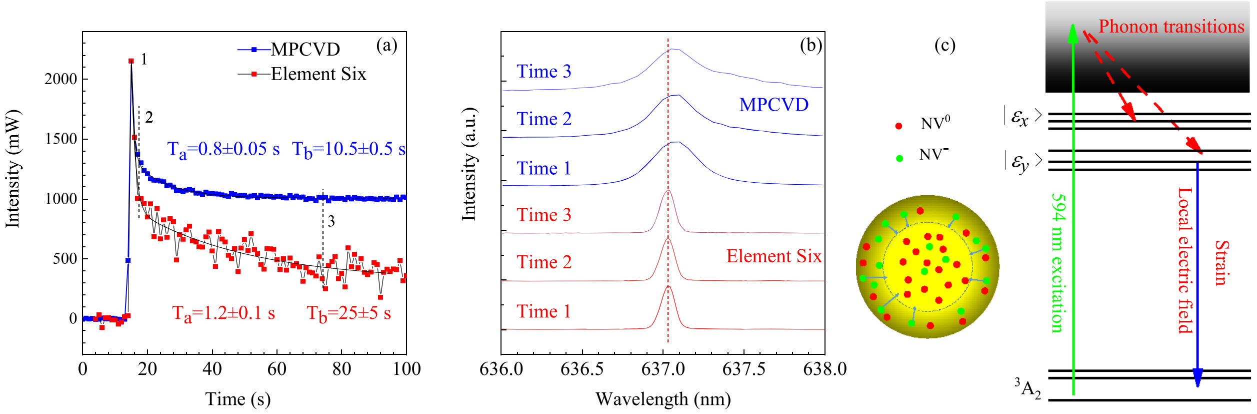

Figure 4. Evolution of the fluorescence spectrum of the NV$^-$ color centers in the decay process. (a) The decay process of the intensity of the NV$^-$ color centers at 4 K. The defect concentrations are 1 ppm (Element Six) and 100 ppm (MPCVD). (b) The spectra diffusion in the decay process. "Time *X*" represents different time points in (a); more details are revealed in Figure S6. (c) The energy level structure of the NV$^-$ color center in the decay process. The rapid ionization process induces the local electric field at the center of the spot, which affects the transition environment of the NV color centers.

NV$^-$ in the center of the laser spot so that excitation saturation is likely to occur under high-power excitation. As the temperature increases, the phonon-assisted up-conversion excitation satisfies the closed-loop process in Figure 1b. A new balance between NV^0 and NV$^-$ would be established in the center of the laser spot, and the concentration of NV$^-$ increases continuously with the up-conversion process, and then the linear power dependence appears. The PL spectra of NV^0 show a linear power dependence from 80 to 293 K in Figure 2f, which agrees with the power dependence of ASPL in the phonon-assisted up-conversion process. Therefore, we believe that in the case of relatively high temperatures (above 80 K), NV color centers in the center of the laser spot are in equilibrium.

The PL mechanism of NV^0 at 594 nm excitation has been confirmed that it comes from the phonon-assisted up-conversion process. Next, we discuss the mechanism of the decay dynamics of NV emissions. The PL spectra of the NV color centers excited by the 594 nm laser at 4 K are shown in the inset of Figure 3b. No PL from NV^0 (575 nm) was observed at low temperatures because of no absorption of NV^0 at this wavelength. During the measurement, the PL intensity of NV$^-$ decays on a timescale of tens of seconds and finally reaches a balance with stable intensity. The laser is alternately turned on and off during the decay process to confirm whether the charge state transition at low temperature is a unidirectional process or not. The fluorescence of NV$^-$ centers do not recover, which means that at low temperatures, the transition from NV$^-$ to NV^0 is a unidirectional process. The NV$^-$ at the center of the laser spot quickly releases excess electrons at the moment of excitation and converts to NV^0 as shown in Figure 3a. Finally, almost all the NVs are in the neutral charge state in the center of the laser spot. In the previous report, it is found that the "ionization" may include two processes.[46] They observe a biexponential evolution featuring a much faster charge conversion at early times followed by a much slower, asymptotic transformation toward an equilibrium charge concentration. The earlier rapid decay process corresponds to the ionization process of the NV$^-$ color center, while the longer-time response is connected to the saturation of available charge traps within the probed volume.[46] The ionization process is rapid (10−100 ms), mainly depending on the excitation power,[19] while the slower process is about 0.1−0.5 s, mainly determined by the surrounding defect density. In our experiment, the decay process has clear temperature dependence, as shown in Figure 3c. As the temperature increases, the decay process gradually disappears. Due to the lower time resolution, we cannot analyze the fast ionization process. We found that a double exponential function is needed to fit the decay process. Here, we use T_a and T_b to characterize the supersaturated filling effect of the defect and the free electron diffusion process. The temperature dependence is shown in the inset of Figure 3d. As the temperature increases, both T_a and T_b show decreasing trends. It is not clear what process these two parameters exactly represent in the current study, but we can tentatively propose that the supersaturated filling effect of the defect is related to the unbalanced local charge environment at the center of the laser spot.[46] The trapping of carriers is determined by the available traps around. When the available charge traps are filled, the carriers need to spread out further to be captured. As the temperature increases, the supersaturated filling effect of the defects weakens, and the trapping process of other impurity defects accelerates, resulting in a smaller T_a. The NV$^-$ defects in the center of the laser spot quickly switch into the dark state, but the conversion speed of the part outside the laser spot is relatively slow, so the NV$^-$ states outside the excitation volume will not lose excess electrons. As the temperature increases, the charge state conversion loop is closed, which leads to the balance of the local charge environment of the defect state, and reduces the influence caused by the local electric field. Therefore, T_b may be related to the electron diffusion process. By comparing the PL changes of NV$^-$ under the anti-Stokes excitation (594 nm) and the Stokes excitation (532 nm), as shown in Figure S2, we find that the ZPL of NV$^-$ does not decay over time under Stokes excitation (532 nm). This is consistent with a previous report[22] where the PL of NV$^-$ under 532 nm excitation is also stable. Therefore, it can be confirmed that this phenomenon is only related to the NV charge state transition under anti-Stokes excitation.

In the experiments, we focus on the PL spectra of the two charge states (NV^0 and NV$^-$). However, the other forms of nitrogen impurities in the sample may affect our experimental results. The previous reports[41] have studied the effect of defect concentration on the dynamics of the charge state conversion. In the process of charge state conversion, other types of defects affect the rate of charge state conversion as an external environment but do not directly participate in the process of charge state conversion. To check the generality of this phenomenon, we have performed similar experimental measurements on other two single crystal diamonds, one grown by MPCVD and the other purchased from Element Six. Figures S3 and S4 show the measurement results of three different positions on the Element Six sample and MPCVD sample, respectively. We can observe similar decay processes of PL in both samples. Here, Figure 4a shows the process of PL decay in both samples with different defect concentrations. The defect concentration of the sample from Element Six is much lower than that in the MPCVD sample. By fitting the decay process, we can confirm that the decay time for the MPCVD sample is much shorter. This is consistent with our previous analysis of the charge state conversion mechanism in which the defect concentration only affects the rate of ionization.

In the experiment, another interesting phenomenon was observed as shown in Figure 4b. In addition to the attenuation of the intensity, the spectra diffusion appears simultaneously. It can be inferred that the transition environment of NV^- has changed during the decay process. Figure 4c shows the fine structures of the NV^- energy level. The NV defect in the diamond comprises a nitrogen atom at a lattice site next to a carbon vacancy giving a center with C_{3v} symmetry. The center has an optically allowed transition between an orbital $^3A_2$ ground state and an orbital ^3E excited state.[19] Both the ground and excited states are spin triplets ($S = 1$). Its fine structure has been studied theoretically in detail.[47] Incorporating the strain effect and the spin interaction results in a complex excited state.

In our experiment, with the establishment of the equilibrium state at the laser spot center, spectral diffusion appears. When the laser is on, the ionization of negative charge state NV^- in the center of the spot loses electrons, resulting in a charge gradient in the center of the spot and outside the spot, thereby generating a local electric field. With the balance of charge states, the local electric field disappears. Similar spectral behavior has been previously observed for color centers in h-BN and has been tentatively attributed to the photoconversion process.[37] They believe that this is a complex optical excitation dynamic and speculate that the spectral diffusion may result from slowly fluctuating, trapped carrier-induced Stark shifts or one-directional photoconversion changes. There are three possible mechanisms, including charge state distribution changes, the population change of adjacent charge traps, or reversible photoconversion processes. In our experiment, we simultaneously observed the spectral diffusion and the emission changes from the different charge states. Under anti-Stokes excitation, the charge state transition is a unidirectional process. The negative charge state NV^- loses electrons and transforms into the neutral charge state NV^0, accompanied by free electrons being trapped by the surrounding traps. Under Stokes excitation, the charge state transition is a reversible process, which contains ionization and recombination. We believe that these three mechanisms may exist simultaneously in the charge state transition process of the NV centers. In comparison, population/depopulation of a charge trap adjacent to the emitter is the most reported across several different quantum systems hosted in wide-bandgap solids.[35,48,49] Random cycling of local electric fields results in large shifts of the ZPL of the emitter through the Stark shift effect. In Figure S5, we show more measurement results of the low-concentration sample (Element Six) and high-concentration sample (MPCVD). For the reason of inhomogeneous spectral diffusion, we believe that at different regions in the spot, the direction of the electric field will be different concerning the crystallographic axis, which results in inhomogeneity. In Figure S6, we show the PL linewidth under Stokes and anti-Stokes excitation at different temperatures. We found that the linewidth under anti-Stokes excitation is smaller than that under Stokes excitation from 80 to 250 K. When the phonon-assisted up-conversion process works, it affects the luminescence process of the color center. However, we think that the process is quite complicated, especially the sample differences. In high-concentration diamond samples, the residual stress is stronger, and the evolution of the spectrum has a certain degree of dependence on the position, which is more complicated and requires more research.

CONCLUSIONS

Here, we report an alternative method to manipulate the reversible conversion between the NV^0 and NV^- in diamond by using phonon-assisted up-conversion excitation. We demonstrate the phonon-assisted PL up-conversion process from the NV^0 center in diamond by studying the temperature and laser power dependence from NV centers. As the temperature increases, the ASPL process of NV^0 becomes stronger, and an abnormally enhanced PL from the NV^- charge state is observed. Also, we observe a fluorescence decay process up to tens of seconds, accompanied by spectral diffusion. We propose that this anomalous behavior is due to the phonon-assisted excitation of the NV^0 color center, which completes the transition from the ground state to the excited state and establishes a new equilibrium of charge states. For the slow evolution of the PL spectra, we believe that it may originate from the local electric field generated by the ionization of the NV^-, which tunes the excited states. Color centers in wide-bandgap semiconductors are generally used in quantum information processing, quantum sensing, and quantum networks due to their excellent optical properties and long spin coherence time. A specific charge state needs to be selected for different application environments, and the manipulation of the charge state is a major issue that must be solved. We believe that this method not only is suitable for NV centers in diamond[50] but also could be used in other defects in diamond and even defects in other systems such as SiC.[51−53] In addition, the demonstrated phonon-assisted up-conversion of NV centers also provides a possibility to achieve the laser cooling of the diamond.[54]

EXPERIMENTAL METHODS

Sample Preparation. The diamond sample was homoepitaxially grown on a high-pressure and high-temperature Ib diamond substrate by microwave plasma-enhanced chemical vapor deposition. The detailed growth process has been depicted elsewhere.[26] Briefly, the precursors used for the growth of the diamond were CH_4 and H_2. The pressure in the growth chamber was nearly 330 mbar, and the substrate temperature was nearly 950 °C. After growth, the CVD diamond sample was removed from the substrate by laser cutting and then used for optical measurements.

Optical Measurements. Stokes PL and ASPL measurements on diamond samples were undertaken in backscattering geometry with a Jobin-Yvon HR800 system equipped with a liquid nitrogen-cooled charge-coupled detector. The ASPL measurements were undertaken with a 100× objective lens (NA = 0.9) and 600 line mm^{-1} grating at room temperature, while a 50× long-working-distance objective lens (NA = 0.5) was used at low temperature. A Montana cryostat system was employed to cool the samples down to 4 from 300 K with a vacuum of 0.4 mTorr. The Stokes and anti-Stokes processes were excited by 594 and 532 nm lasers, respectively. During the experiment, the spectra change slowly with time, and we used time-based spectral scanning to measure until the charge state was balanced. In Figure S1 of the Supporting Information, we show how to obtain the intensity of ZPL and total PL spectra of the NV centers.

■ ASSOCIATED CONTENT

Supporting Information

The Supporting Information is available free of charge at https://pubs.acs.org/doi/10.1021/acsphotonics.1c01928.

> Detailed experimental and analytical procedures; spectral intensity analysis; charge dynamics; generality of the results; estimation of photo-ionization-induced electric field; linewidth comparison between Stokes and anti-Stokes excitation (PDF)

■ AUTHOR INFORMATION

Corresponding Authors

Chong-Xin Shan − *Henan Key Laboratory of Diamond Optoelectronic Materials and Devices, Key Laboratory of Material Physics, Ministry of Education, School of Physics and Microelectronics, Zhengzhou University, Zhengzhou 450052, People's Republic of China*; Email: cxshan@zzu.edu.cn

Jun Zhang − *State Key Laboratory of Superlattices and Microstructures, Institute of Semiconductors, & Center of Materials Science and Optoelectronics Engineering, University of Chinese Academy of Sciences, Chinese Academy of Sciences, Beijing 100083, People's Republic of China*; orcid.org/0000-0002-9831-6796; Email: zhangjwill@semi.ac.cn

Authors

Yuan-Fei Gao − *State Key Laboratory of Superlattices and Microstructures, Institute of Semiconductors, & Center of Materials Science and Optoelectronics Engineering, University of Chinese Academy of Sciences, Chinese Academy of Sciences, Beijing 100083, People's Republic of China; Beijing Academy of Quantum Information Sciences, Beijing 100193, People's Republic of China*; orcid.org/0000-0001-5455-5421

Jia-Min Lai − *State Key Laboratory of Superlattices and Microstructures, Institute of Semiconductors, & Center of Materials Science and Optoelectronics Engineering, University of Chinese Academy of Sciences, Chinese Academy of Sciences, Beijing 100083, People's Republic of China*

Yu-Jia Sun − *State Key Laboratory of Superlattices and Microstructures, Institute of Semiconductors, & Center of Materials Science and Optoelectronics Engineering, University of Chinese Academy of Sciences, Chinese Academy of Sciences, Beijing 100083, People's Republic of China*

Xue-Lu Liu − *State Key Laboratory of Superlattices and Microstructures, Institute of Semiconductors, & Center of Materials Science and Optoelectronics Engineering, University of Chinese Academy of Sciences, Chinese Academy of Sciences, Beijing 100083, People's Republic of China*; orcid.org/0000-0001-9156-6760

Chao-Nan Lin − *Henan Key Laboratory of Diamond Optoelectronic Materials and Devices, Key Laboratory of Material Physics, Ministry of Education, School of Physics and Microelectronics, Zhengzhou University, Zhengzhou 450052, People's Republic of China*

Ping-Heng Tan − *State Key Laboratory of Superlattices and Microstructures, Institute of Semiconductors, & Center of Materials Science and Optoelectronics Engineering, University of Chinese Academy of Sciences, Chinese Academy of Sciences, Beijing 100083, People's Republic of China*; orcid.org/0000-0001-6575-1516

Complete contact information is available at: https://pubs.acs.org/10.1021/acsphotonics.1c01928

Funding

We acknowledge support from the National Key Research and Development Program of China (2017YFA0303401), the CAS Interdisciplinary Innovation Team, the Strategic Priority Research Program of Chinese Academy of Sciences (grant no. XDB28000000), and the NSFC (12074371, U21A2070, and 62027816).

Notes

The authors declare no competing financial interest.

■ REFERENCES

(1) Tetienne, J. P.; Dontschuk, N.; Broadway, D. A.; Stacey, A.; Simpson, D. A.; Hollenberg, L. C. L. Quantum imaging of current flow in graphene. *Sci. Adv.* **2017**, *3*, No. e1602429.

(2) Rose, B. C.; Huang, D.; Zhang, Z. H.; Stevenson, P.; Tyryshkin, A. M.; Sangtawesin, S.; Srinivasan, S.; Loudin, L.; Markham, M. L.; Edmonds, A. M.; Twitchen, D. J.; Lyon, S. A.; de Leon, N. P. Observation of an environmentally insensitive solid-state spin defect in diamond. *Science* **2018**, *361*, 60−63.

(3) Zheng, H. J.; Sun, Z. Y.; Chatzidrosos, G.; Zhang, C.; Nakamura, K.; Sumiya, H.; Ohshima, T.; Isoya, J.; Wrachtrup, J.; Wickenbrock, A.; Budker, D. Microwave-Free Vector Magnetometry with Nitrogen-Vacancy Centers along a Single Axis in Diamond. *Phys. Rev. Appl.* **2020**, *13*, No. 022338.

(4) Balasubramanian, G.; Neumann, P.; Twitchen, D.; Markham, M.; Kolesov, R.; Mizuochi, N.; Isoya, J.; Achard, J.; Beck, J.; Tissler, J.; Jacques, V.; Hemmer, P. R.; Jelezko, F.; Wrachtrup, J. Ultralong spin coherence time in isotopically engineered diamond. *Nat. Mater.* **2009**, *8*, 383−387.

(5) Jelezko, F.; Gaebel, T.; Popa, I.; Domhan, M.; Gruber, A.; Wrachtrup, J. Observation of coherent oscillation of a single nuclear spin and realization of a two-qubit conditional quantum gate. *Phys. Rev. Lett.* **2004**, *93*, No. 130501.

(6) Li, P. B.; Xiang, Z. L.; Rabl, P.; Nori, F. Hybrid Quantum Device with Nitrogen-Vacancy Centers in Diamond Coupled to Carbon Nanotubes. *Phys. Rev. Lett.* **2016**, *117*, No. 015502.

(7) Lo Piparo, N.; Razavi, M.; Munro, W. J. Measurement-device-independent quantum key distribution with nitrogen vacancy centers in diamond. *Phys. Rev. A* **2017**, *95*, No. 022338.

(8) Bhaumik, A.; Sachan, R.; Narayan, J. Tunable charge states of nitrogen-vacancy centers in diamond for ultrafast quantum devices. *Carbon* **2019**, *142*, 662−672.

(9) Michl, J.; Teraji, T.; Zaiser, S.; Jakobi, I.; Waldherr, G.; Dolde, F.; Neumann, P.; Doherty, M. W.; Manson, N. B.; Isoya, J.; Wrachtrup, J. Perfect alignment and preferential orientation of

nitrogen-vacancy centers during chemical vapor deposition diamond growth on (111) surfaces. *Appl. Phys. Lett.* **2014**, *104*, 102407.

(10) Sangtawesin, S.; Brundage, T. O.; Atkins, Z. J.; Petta, J. R. Highly tunable formation of nitrogen-vacancy centers via ion implantation. *Appl. Phys. Lett.* **2014**, *105*, No. 063107.

(11) Reineck, P.; Capelli, M.; Lau, D. W.; Jeske, J.; Field, M. R.; Ohshima, T.; Greentree, A. D.; Gibson, B. C. Bright and photostable nitrogen-vacancy fluorescence from unprocessed detonation nanodiamond. *Nanoscale* **2017**, *9*, 497−502.

(12) Acosta, V. M.; Bauch, E.; Ledbetter, M. P.; Santori, C.; Fu, K. M. C.; Barclay, P. E.; Beausoleil, R. G.; Linget, H.; Roch, J. F.; Treussart, F.; Chemerisov, S.; Gawlik, W.; Budker, D. Diamonds with a high density of nitrogen-vacancy centers for magnetometry applications. *Phys. Rev. B* **2009**, *80*, No. 115202.

(13) Khomich, A. A.; Kudryavtsev, O. S.; Bolshakov, A. P.; Khomich, A. V.; Ashkinazi, E. E.; Ralchenko, V. G.; Vlasov, I. I.; Konov, V. I. Use of Optical Spectroscopy Methods to Determine the Solubility Limit for Nitrogen in Diamond Single Crystals Synthesized by Chemical Vapor Deposition. *J. Appl. Spectrosc.* **2015**, *82*, 242−247.

(14) Osswald, S.; Yushin, G.; Mochalin, V.; Kucheyev, S. O.; Gogotsi, Y. Control of sp(2)/sp(3) carbon ratio and surface chemistry of nanodiamond powders by selective oxidation in air. *J. Am. Chem. Soc.* **2006**, *128*, 11635−11642.

(15) Orwa, J. O.; Santori, C.; Fu, K. M. C.; Gibson, B.; Simpson, D.; Aharonovich, I.; Stacey, A.; Cimmino, A.; Balog, P.; Markham, M.; Twitchen, D.; Greentree, A. D.; Beausoleil, R. G.; Prawer, S. Engineering of nitrogen-vacancy color centers in high purity diamond by ion implantation and annealing. *J. Appl. Phys.* **2011**, *109*, No. 083530.

(16) Hauf, M. V.; Grotz, B.; Naydenov, B.; Dankerl, M.; Pezzagna, S.; Meijer, J.; Jelezko, F.; Wrachtrup, J.; Stutzmann, M.; Reinhard, F.; Garrido, J. A. Chemical control of the charge state of nitrogen-vacancy centers in diamond. *Phys. Rev. B* **2011**, *83*, No. 081304.

(17) Kato, H.; Wolfer, M.; Schreyvogel, C.; Kunzer, M.; Muller-Sebert, W.; Obloh, H.; Yamasaki, S.; Nebel, C. Tunable light emission from nitrogen-vacancy centers in single crystal diamond PIN diodes. *Appl. Phys. Lett.* **2013**, *102*, 151101.

(18) Grotz, B.; Hauf, M. V.; Dankerl, M.; Naydenov, B.; Pezzagna, S.; Meijer, J.; Jelezko, F.; Wrachtrup, J.; Stutzmann, M.; Reinhard, F.; Garrido, J. A. Charge state manipulation of qubits in diamond. *Nat. Commun.* **2012**, *3*, 729.

(19) Aslam, N.; Waldherr, G.; Neumann, P.; Jelezko, F.; Wrachtrup, J. Photo-induced ionization dynamics of the nitrogen vacancy defect in diamond investigated by single-shot charge state detection. *New J. Phys.* **2013**, *15*, 13064−13080.

(20) Kaviani, M.; Deak, P.; Aradi, B.; Frauenheim, T.; Chou, J. P.; Gali, A. Proper Surface Termination for Luminescent Near-Surface NV Centers in Diamond. *Nano Lett.* **2014**, *14*, 4772−4777.

(21) Chou, J. P.; Retzker, A.; Gali, A. Nitrogen-Terminated Diamond (111) Surface for Room-Temperature Quantum Sensing and Simulation. *Nano Lett.* **2017**, *17*, 2294−2298.

(22) Beha, K.; Batalov, A.; Manson, N. B.; Bratschitsch, R.; Leitenstorfer, A. Optimum Photoluminescence Excitation and Recharging Cycle of Single Nitrogen-Vacancy Centers in Ultrapure Diamond. *Phys. Rev. Lett.* **2012**, *109*, No. 097404.

(23) Han, K. Y.; Kim, S. K.; Eggeling, C.; Hell, S. W. Metastable Dark States Enable Ground State Depletion Microscopy of Nitrogen Vacancy Centers in Diamond with Diffraction-Unlimited Resolution. *Nano Lett.* **2010**, *10*, 3199−3203.

(24) Ji, P.; Dutt, M. V. G. Charge state dynamics of the nitrogen vacancy center in diamond under 1064-nm laser excitation. *Phys. Rev. B* **2016**, *94*, No. 024101.

(25) Zhang, J.; Li, D. H.; Chen, R. J.; Xiong, Q. H. Laser cooling of a semiconductor by 40 kelvin. *Nature* **2013**, *493*, 504−508.

(26) Gao, Y.-F.; Tan, Q. H.; Liu, X.-L.; Ren, S.-L.; Sun, Y.-J.; Meng, D.; Lu, Y.-J.; Tan, P.-H.; Shan, C.-X.; Zhang, J. Phonon-Assisted Photoluminescence Up-Conversion of Silicon-Vacancy Centers in Diamond. *J. Phys. Chem. Lett.* **2018**, *9*, 6656−6661.

(27) Zhang, J.; Zhang, Q.; Wang, X. Z.; Kwek, L. C.; Xiong, Q. H. Resolved-sideband Raman cooling of an optical phonon in semiconductor materials. *Nat. Photonics* **2016**, *10*, 600−605.

(28) Sweeney, T. M.; Carter, S. G.; Bracker, A. S.; Kim, M.; Kim, C. S.; Yang, L.; Vora, P. M.; Brereton, P. G.; Cleveland, E. R.; Gammon, D. Cavity-stimulated Raman emission from a single quantum dot spin. *Nat. Photonics* **2014**, *8*, 442−447.

(29) Evans, C. L.; Potma, E. O.; Puoris'haag, M.; Cote, D.; Lin, C. P.; Xie, X. S. Chemical imaging of tissue in vivo with video-rate coherent anti-Stokes Raman scattering microscopy. *Proc. Natl. Acad. Sci. U. S. A.* **2005**, *102*, 16807−16812.

(30) Atature, M.; Englund, D.; Vamivakas, N.; Lee, S. Y.; Wrachtrup, J. Material platforms for spin-based photonic quantum technologies. *Nat. Rev. Mater.* **2018**, *3*, 38−51.

(31) Sallen, G.; Tribu, A.; Aichele, T.; Andre, R.; Besombes, L.; Bougerol, C.; Richard, M.; Tatarenko, S.; Kheng, K.; Poizat, J. P. Subnanosecond spectral diffusion measurement using photon correlation. *Nat. Photonics* **2010**, *4*, 696−699.

(32) Pan, J. W.; Chen, Z. B.; Lu, C. Y.; Weinfurter, H.; Zeilinger, A.; Zukowski, M. Multiphoton entanglement and interferometry. *Rev. Mod. Phys.* **2012**, *84*, 777−838.

(33) Greentree, A. D.; Olivero, P.; Draganski, M.; Trajkov, E.; Rabeau, J. R.; Reichart, P.; Gibson, B. C.; Rubanov, S.; Huntington, S. T.; Jamieson, D. N.; Prawer, S. Critical components for diamond-based quantum coherent devices. *J. Phys.: Condens. Matter* **2006**, *18*, S825−S842.

(34) Bradac, C.; Gao, W.; Forneris, J.; Trusheim, M. E.; Aharonovich, I. Quantum nanophotonics with group IV defects in diamond. *Nat. Commun.* **2019**, *10*, 5625.

(35) Anderson, C. P.; Bourassa, A.; Miao, K. C.; Wolfowicz, G.; Mintun, P. J.; Crook, A. L.; Abe, H.; Ul Hassan, J.; Son, N. T.; Ohshima, T.; Awschalom, D. D. Electrical and optical control of single spins integrated in scalable semiconductor devices. *Science* **2019**, *366*, 1225−1230.

(36) Tamarat, P.; Gaebel, T.; Rabeau, J. R.; Khan, M.; Greentree, A. D.; Wilson, H.; Hollenberg, L. C. L.; Prawer, S.; Hemmer, P.; Jelezko, F.; Wrachtrup, J. Stark shift control of single optical centers in diamond. *Phys. Rev. Lett.* **2006**, *97*, No. 083002.

(37) Tran, T. T.; Bradac, C.; Solntsev, A. S.; Toth, M.; Aharonovich, I. Suppression of Spectral Diffusion by Anti-Stokes Excitation of Quantum Emitters in Hexagonal Boron Nitride. *Appl. Phys. Lett.* **2019**, *115*, No. 071101.

(38) Wang, J.-F.; Yan, F.-F.; Li, Q.; Liu, Z.-H.; Cui, J.-M.; Liu, Z.-D.; Gali, A.; Xu, J.-S.; Li, C.-F.; Guo, G.-C. Robust coherent control of solid-state spin qubits using anti-Stokes excitation. *Nat. Commun.* **2021**, *12*, 3223.

(39) Waldherr, G.; Beck, J.; Steiner, M.; Neumann, P.; Gali, A.; Frauenheim, T.; Jelezko, F.; Wrachtrup, J. Dark States of Single Nitrogen-Vacancy Centers in Diamond Unraveled by Single Shot NMR. *Phys. Rev. Lett.* **2011**, *106*, No. 157601.

(40) Clark, C. D.; Kanda, H.; Kiflawi, I.; Sittas, G. Silicon defects in diamond. *Phys. Rev. B* **1995**, *51*, 16681−16688.

(41) Dhomkar, S.; Jayakumar, H.; Zangara, P. R.; Meriles, C. A. Charge Dynamics in near-Surface, Variable-Density Ensembles of Nitrogen-Vacancy Centers in Diamond. *Nano Lett.* **2018**, *18*, 4046−4052.

(42) Wang, K.-Y.; Guo, R.-A.; Wang, H.-X. Temperature dependence of nitrogen-vacancy optical center in diamond. *Acta Phys. Sin.* **2020**, *69*, 127802.

(43) Venkateswarlu, K. Temperature Dependence of the Intensities of Raman Lines. *Nature* **1947**, *159*, 96−97.

(44) Anderson, C. P.; Glen, E. O.; Zeledon, C.; Bourassa, A.; Jin, Y.; Zhu, Y.; Vorwerk, C.; Crook, A. L.; Abe, H.; Ul-Hassan, J.; Ohshima, T.; Son, N. T.; Galli, G.; Awschalom, D. D. Five-second coherence of a single spin with single-shot readout in silicon carbide. *Sci. Adv.* **2022**, *8*, No. eabm5912.

(45) Hacquebard, L.; Childress, L. Charge-state dynamics during excitation and depletion of the nitrogen-vacancy center in diamond. *Phys. Rev. A* **2018**, *97*, No. 063408.

(46) Dhomkar, S.; Zangara, P. R.; Henshaw, J.; Meriles, C. A. On-Demand Generation of Neutral and Negatively Charged Silicon-Vacancy Centers in Diamond. *Phys. Rev. Lett.* **2018**, *120*, No. 117401.

(47) Maze, J. R.; Gali, A.; Togan, E.; Chu, Y.; Trifonov, A.; Kaxiras, E.; Lukin, M. D. Properties of nitrogen-vacancy centers in diamond: the group theoretic approach. *New J. Phys.* **2011**, *13*, 780−782.

(48) Neitzke, O.; Morfa, A.; Wolters, J.; Schell, A. W.; Kewes, G.; Benson, O. Investigation of Line Width Narrowing and Spectral Jumps of Single Stable Defect Centers in ZnO at Cryogenic Temperature. *Nano Lett.* **2015**, *15*, 3024−3029.

(49) Wolters, J.; Sadzak, N.; Schell, A. W.; Schroder, T.; Benson, O. Measurement of the Ultrafast Spectral Diffusion of the Optical Transition of Nitrogen Vacancy Centers in Nano-Size Diamond Using Correlation Interferometry. *Phys. Rev. Lett.* **2013**, *110*, No. 027401.

(50) Lühmann, T.; Küpper, J.; Dietel, S.; Staacke, R.; Meijer, J.; Pezzagna, S. Charge-State Tuning of Single SnV Centers in Diamond. *ACS Photonics* **2020**, *7*, 3376−3385.

(51) Wolfowicz, G.; Anderson, C. P.; Yeats, A. L.; Whiteley, S. J.; Niklas, J.; Poluektov, O. G.; Heremans, F. J.; Awschalom, D. D. Optical charge state control of spin defects in 4H-SiC. *Nat. Commun.* **2017**, *8*, 1876.

(52) Morioka, N.; Babin, C.; Nagy, R.; Gediz, I.; Hesselmeier, E.; Liu, D.; Joliffe, M.; Niethammer, M.; Dasari, D.; Vorobyov, V.; Kolesov, R.; Stohr, R.; Ul-Hassan, J.; Son, N. T.; Ohshima, T.; Udvarhelyi, P.; Thiering, G.; Gali, A.; Wrachtrup, J.; Kaiser, F. Spin-controlled generation of indistinguishable and distinguishable photons from silicon vacancy centres in silicon carbide. *Nat. Commun.* **2020**, *11*, 2516.

(53) Koehl, W. F.; Buckley, B. B.; Heremans, F. J.; Calusine, G.; Awschalom, D. Room temperature coherent control of defect spin qubits in silicon carbide. *Nature* **2011**, *479*, 84−87.

(54) Kern, M.; Jeske, J.; Lau, D. W. M.; Greentree, A. D.; Jelezko, F.; Twamley, J. Optical cryocooling of diamond. *Phys. Rev. B* **2017**, *95*, No. 235306.